Optical Materials 50 (2015) 128–133

Contents lists available at ScienceDirect

Optical Materials

journal homepage: www.elsevier.com/locate/optmat

Study of structural, optical and photoluminescence properties of indium-doped zinc sulfide thin films for optoelectronic applications

Abdelhak Jrad *, Tarek Ben Nasr, Najoua Turki-Kamoun

Laboratoire de Physique de la Matière Condensée, Faculté des Sciences de Tunis, Université Tunis El Manar, 2092 Tunis, Tunisia

ARTICLE INFO

Article history:
Received 25 July 2015
Received in revised form 12 October 2015
Accepted 12 October 2015
Available online 21 October 2015

Keywords:
CBD
ZnS
Spitzer–Fan model
Wemple–DiDomenico model
Photoluminescence

ABSTRACT

In the present work, we have deposited indium-doped zinc sulfide (ZnS:In) thin films by chemical bath deposition technique (CBD). The structural properties studied by X-ray diffraction indicate that ZnS:In has a cubic structure with an average crystallite size 4.7–11.0 nm. Transmission and reflection spectra reveal the presence of interference fringes indicating thickness uniformity and surface homogeneity of deposited material. All the films were transparent in the visible and infrared regions ($\geqslant$60%), which allows us to use this material as an optical window or a buffer layer in solar cells. The obtained band gap energy E_g is in the range of 3.70–3.76 eV. The refractive index and thickness of ZnS:In thin films was calculated using envelope method. The variation of the refractive index along the Cauchy distribution was observed in all ZnS:In thin films. The analysis of the refractive index data through the Wemple–DiDomenico model leads to the single oscillator energy (E_0) and the dispersion energy (E_d).

1. Introduction

Zinc sulfide (ZnS) attract a great interest in material science because of their wide range of applications like buffer layer for solar cells [1–4] dielectric optical filters [5], light emitting devices [6], spintronic devices [7], electroluminescent devices, photodetectors, biosensors [8], gas sensors, chemical sensors and nanogenerators [9]. Furthermore, ZnS thin films show n-type conduction, crystallizes into cubic or hexagonal structure and can be prepared using different techniques such as thermal evaporation [10], chemical vapor deposition [11], spray pyrolysis [12] and chemical bath deposition [13]. Among these methods, chemical bath deposition technique (CBD) is one of the simplest and most cost effective methods of thin film deposition especially when large area deposition is required. In the present work, CBD technique is used for the deposition of ZnS:In thin layers. In our knowledge no reports have investigated structural, optical and photoluminescence properties of In-doped ZnS thin films elaborated by CBD. So the main contribution of this study is to investigate the influence of In-doping on the structural, optical and photoluminescence properties of ZnS thin films elaborated by CBD. To characterize In-doped ZnS thin films, we used many experimental techniques such as X-ray diffraction (XRD), spectrophotometer and fluorescence spectrometer. Besides, Wemple–DiDomineco model was used to describe the dielectric response for transitions below the optical gap [14]. Only, few papers applied this model for zinc sulfide thin films [15]. Same result was found by Bakr et al. [16], Bhuiyan et al. [17], Murali [18] and Jrad et al. [19].

In the present work, we report the chemical bath deposition of undoped and In-doped ZnS thin films and their characterization. The effect of dopant concentration on structural, optical and photoluminescence properties of these films is investigated in order to use it as a buffer layer or optical window in photovoltaic devices.

2. Experimental

Indium doped zinc sulfide thin films are prepared on glass substrate using chemical bath deposition technique. The aqueous solution contains zinc sulfate ($ZnSO_4{\cdot}7H_2O$; $\geqslant$99.0%) and thiourea ($SC(NH_2)_2$; >99.0%). Indium chloride ($InCl_3$; 98%) is used as a doping agent. All the reagents were supplied by Sigma–Aldrich Chemicals. The ZnS include three successive layers [20], each of them being elaborated with a deposition time of 90 min. The ZnS bath solutions are maintained at 80 °C and continuously stirred in order to ensure homogeneous distribution of the chemical compounds [21]. The experimental setup was explained with more details by Ben Nasr et al. [22]. Indium atomic concentration ($y = [In^{3+}]/[Zn^{2+}]$) in the solution is varied from 0 to 10 at.%. The X-ray diffraction (XRD) patterns were recorded with an automated Bruker D8 advance diffractometer, operated at 35 kV and 35 mA, using the copper Kα radiation (λ = 1.54056 Å) in the 2θ range 20–60° with

* Corresponding author.
E-mail address: abdelhak.jrad@gmail.com (A. Jrad).

http://dx.doi.org/10.1016/j.optmat.2015.10.011
0925-3467/

a step size of 0.0300° and a time per step of 13.32 s. Transmission and reflection data of the films were collected from 250 to 2500 nm wavelength with Perkin–Elmer Lambda 950 spectrophotometer at room temperature. Photoluminescence spectra were recorded at room temperature from 300 to 650 nm using Perkin–Elmer LS55 spectrometer with xenon flash lamp as a source of excitation. All PL emission spectra were recorded at 300 nm excitation with scanning speed 400 nm/min. The PL intensity is measured at a 90° angle relative to the excitation light. The cut-off (filter) selected is 350 nm. The data were analyzed using the FL Winlab software.

3. Results and discussion

3.1. Structural analysis

The effect of indium concentration on the X-ray diffraction patterns of the zinc sulfide thin films is shown in Fig. 1. It should be noted that, the intensity of the diffraction peak increases with the increasing dopant concentration until 6 at.%, then decreases, revealing degradation of film crystallinity. The crystallite size (D) is calculated using Scherrer's formula [23]:

$$D = \frac{0.9\lambda}{\sqrt{\beta^2 - \beta_0^2}\cos(\theta)} \quad (1)$$

where λ, θ, β and β_0 are the X-ray wavelength, Bragg diffraction angle, the experimental full-width at half-maximum (FWHM) and the width of the corresponding peak due to the instrumental expansion, which is about 0.125° [24] respectively. The crystallite size (D) initially increased from 7.1 nm to 14.3 nm in the dopant concentration range 0–6 at.% and decreased to 9.5 nm with further increase of the dopant concentration to 10 at.%. The crystallite size values of ZnS layers obtained in this work are matched with the reported values by Nagamani et al. [25].

Using grain size values, the dislocation density (δ_{dis}), defined as the length of dislocation lines per unit volume of the crystal are calculated using the Williamson and Smallman's formula [24]:

$$\delta_{dis} = \frac{1}{D^2} \quad (2)$$

The dislocation density (δ_{dis}) initially decreased from 19.73×10^9 lignes mm^{-2} to 4.92×10^9 lignes mm^{-2} in the dopant concentration range 0–6 at.% and increased to 11.08×10^9 lignes mm^{-2} with further increase of the dopant concentration to 10 at.%. This behavior can be explained by the change of the crystallite size (D) with dopant concentration. Ajili and Kamoun [24] reported similar observations for β-$In_{2-x}Al_xS_3$ thin films.

The microstrain (ε) which is an interesting structural parameter, is calculated using the following relation [26]:

$$\epsilon = \frac{\beta\cos(\theta)}{4} \quad (3)$$

where β is the full-width at half maximum of (1 1 1) peak and θ is the Bragg diffraction angle. The variation of the microstrain (ε) and crystallite size (D) with the dopant concentration are presented in Fig. 2. ZnS: 6 at.% In thin film has the largest crystallite size and the least strain.

3.2. Optical properties

3.2.1. Transmittance and reflectance spectra

Transmittance and reflectance spectra of indium doped zinc sulfide thin films are shown in Fig. 3. Interference fringes are observed in the visible region for all the dopant concentrations. The presence of interference fringes indicates thickness uniformity and surface homogeneity of deposited material. From Fig. 3 is noticed that the ZnS:In thin films has higher transmittance values in the visible and infrared regions, the optical transparency of the films varies between 50% and 70%. In addition, the values of the reflectance for all the films are in the range 20–40%, which allows us to use this material as an optical window or a buffer layer in solar cells.

3.2.2. Band gap energy (E_g)

The band gap energy (E_g) is determined using the differential reflectance spectra of the films [27]. As it can be seen in Fig. 4 the band gap energy is slightly affected by the dopant concentration. The estimated band gap energy varies in the range 3.70–3.76 eV (Table 1) when the dopant concentration varies from 0 to

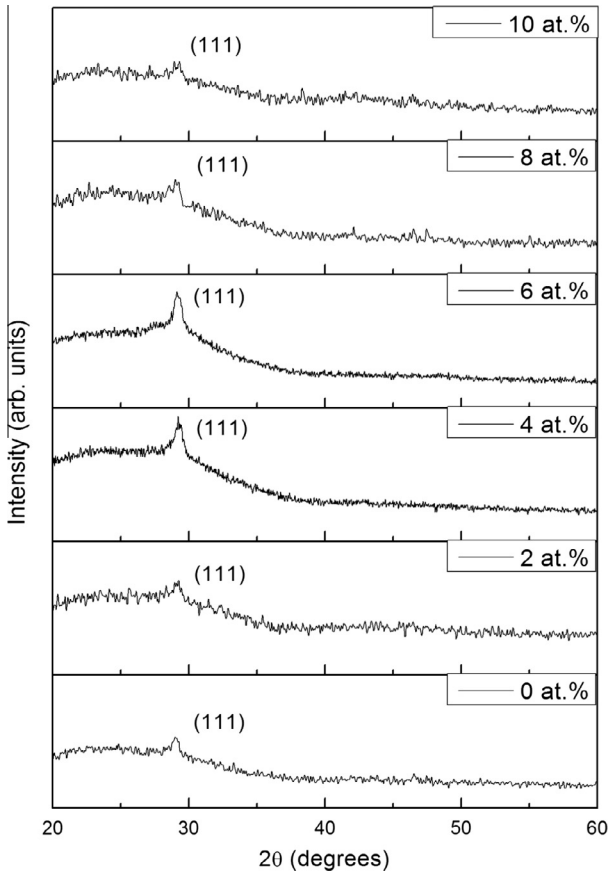

Fig. 1. X-ray diffraction patterns of undoped and In-doped ZnS thin films for different ratios $\left(0 \leqslant y = \frac{[In^{3+}]}{[Zn^{2+}]} \leqslant 10\ \text{at.}\%\right)$.

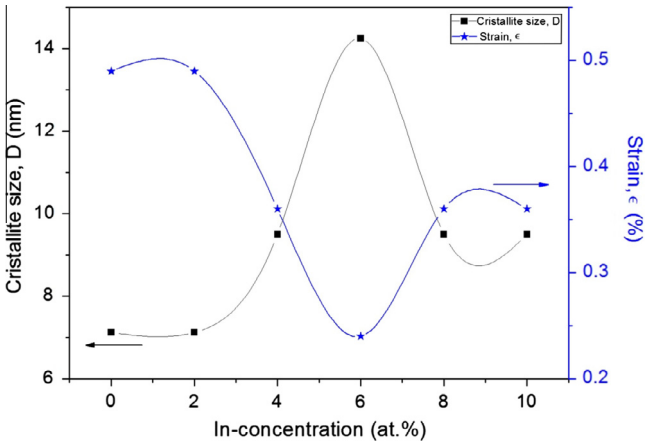

Fig. 2. The variation of crystallite size, D, and residual stress, ε, for different In inclusions $\left(0 \leqslant y = \frac{[In^{3+}]}{[Zn^{2+}]} \leqslant 10\ \text{at.}\%\right)$.